AAPS PharmSciTech (2024) 25:110
https://doi.org/10.1208/s12249-024-02826-6

RESEARCH ARTICLE

LL37 Microspheres Loaded on Activated Carbon-chitosan Hydrogel: Anti-bacterial and Anti-toxin Wound Dressing for Chronic Wound Infections

Bee-Yee Lim[1,2] · Fazren Azmi[2] · Shiow-Fern Ng[2]

Received: 15 November 2023 / Accepted: 29 April 2024 / Published online: 13 May 2024

Abstract

Antimicrobial peptide LL37 is a promising antibacterial candidate due to its potent antimicrobial activity with no known bacterial resistance. However, intrinsically LL37 is susceptible to degradation in wound fluids limits its effectiveness. Bacterial toxins which are released after cell lysis are found to hinder wound healing. To address these challenges, encapsulating LL37 in microspheres (MS) and loading the MS onto activated carbon (AC)-chitosan (CS) hydrogel. This advanced wound dressing not only protects LL37 from degradation but also targets bacterial toxins, aiding in the healing of chronic wound infections. First, LL37 MS and LL37-AC-CS hydrogel were prepared and characterised in terms of physicochemical properties, drug release, and peptide-polymer compatibility. Antibacterial and antibiofilm activity, bacterial toxin elimination, cell migration, and cell cytotoxicity activities were investigated. LL37-AC-CS hydrogel was effective against *Escherichia coli, Pseudomonas aeruginosa*, and *Staphylococcus aureus*. LL37-AC-CS hydrogel bound more endotoxin than AC with CS hydrogel alone. The hydrogel also induced cell migration after 72 h and showed no cytotoxicity towards NHDF after 72 h of treatment. In conclusion, the LL37-AC-CS hydrogel was shown to be a stable, non-toxic advanced wound dressing method with enhanced antimicrobial and antitoxin activity, and it can potentially be applied to chronic wound infections to accelerate wound healing.

Keywords antimicrobial peptide LL37 · activated carbon · bacterial toxins · infected wound · wound healing

Introduction

In recent years, the rise in wound infections has emerged as a leading cause of mortality among critically ill individuals admitted to hospitals, particularly in long-term care settings. Managing these infections has imposed a substantial strain on the healthcare system [1]. Numerous antibacterial substances have been documented to exhibit bacterial resistance and cross-resistance. Opportunistic pathogens, like *Pseudomonas aeruginosa* and *Staphylococcus aureus*, can effectively colonise skin wounds and create biofilms [2–4]. The elimination of these bacteria poses a significant challenge predominantly from the constrained efficacy of antibiotics and host clearance mechanisms, including antibodies and phagocytes, in penetrating the microbial biofilm [5, 6]. Moreover, the release of exotoxins from lysed bacteria exacerbates the mobilization of immune cells, triggering an immoderate and deleterious inflammatory reaction [7].

LL37, an antimicrobial peptide (AMP), has proven effective against multi-drug-resistant microbes [8, 9]. LL37 has demonstrated rapid action with a wide-ranging of antimicrobial efficacy, targeting Gram-positive and Gram-negative bacteria, mycobacteria, viruses, fungi, and protozoa [10, 11]. The amphipathic and cationic characteristics of AMP facilitate robust binding through electrostatic or hydrophobic interactions with the negatively charged lipid membranes of bacteria resulting in membrane disruption [12]. During the wound healing process, LL37 also controls inflammation and chemotactic activity at infected injury sites. It also binds to and neutralizes lipopolysaccharides (LPS, endotoxin) and helps in the reepithelialisation process, ultimately promoting wound closure [13, 14]. Thus, LL37 can be a promising antimicrobial agent for wound infection. However, AMP is susceptible to bacterial proteases, and

✉ Shiow-Fern Ng
nsfern@ukm.edu.my; nsfern@gmail.com

[1] National Pharmaceutical Regulatory Agency, 36, Jalan Profesor Diraja Ungku Aziz, PJS 13, Petaling Jaya, Selangor 46200, Malaysia

[2] Centre for Drug Delivery Technology and Vaccine, Faculty of Pharmacy, Universiti Kebangsaan Malaysia, Kuala Lumpur 50300, Malaysia

endogenous proteases in wound fluids which limits its clinical application. A potential solution is thus loading the AMPs into a microparticulate vehicle to overcome such instability problems.

Apart from infection, the bacteria present in the chronic wounds secrete exotoxins during active proliferation, and endotoxins upon cell lysis or death [15]. These bacterial toxins stimulate the production of local inflammatory mediators and can prolong wound healing [15]. Activated carbon (AC), a highly porous and non-toxic biomaterial, was exploited as an effective antitoxin agent in wound dressing [16]. This current work aims to formulate a multi-action, i.e., antibacterial and antitoxin actions wound dressing formulation for the treatment of chronic wound infection. We propose encapsulating LL37 into poly (D,L-lactic-co-glycolic acid) (PLGA) MS and loading these MS in CS hydrogel containing AC. When this hydrogel formulation is placed on an infected wound, we theorise that the AMP will be released from the MS which in turn kills the bacteria. Upon lysis, toxins released from bacteria on the wound will adsorb onto the AC. This in turn prevents the release of harmful bacterial toxins onto wounds while eradicating bacteria, thus accelerating wound healing. Therefore, this study aims to assess the physicochemical properties as well as its *in vitro* action of the LL37 microspheres loaded into AC with chitosan hydrogel in eliminating bacteria toxins and accelerating chronic wound healing.

Materials and Methods

Materials

LL37 (LLGDFFRKSKEKIGKEFKRIVQRIKDFLRNLVPRTES, molecular mass 4493.37, > 95% purity) was obtained from Bank Peptide (China). Poly (D,L-lactic-co-glycolic acid) (PLGA, MW 7–17 kDa, lactic:glycolic acid 50:50), chitosan (CS, MW 50–190 kDa, degree of deacetylation of 75–85%), 2,3,5-triphenyltetrazolium chloride (TTC), Dulbecco's modified Eagle's medium (DMEM) and antibiotics (streptomycin and penicillin) were procured from Sigma-Aldrich (US). Polyvinyl alcohol (PVA) from R&M Chemicals, Malaysia. Activated carbon (AC) powder was sponsored by Noble Health Sdn. Bhd., Malaysia. Mueller Hinton Agar (MHA) and Mueller Hinton Broth (MHB) from Oxoid (UK). *Staphylococcus aureus* (*S. aureus*) ATCC 25923, *Escherichia coli* (*E. coli*) ATCC 25922, and *Pseudomonas aeruginosa* (*P. aeruginosa*) ATCC 27853 from microbiology laboratory, Faculty of Pharmacy, Universiti Kebangsaan Malaysia (UKM). XTT [2,3-bis(2-methoxy-4-nitro-5-sulfophenyl)-2H-tetrazolium-5-carboxanilide] was procured from Nacalai Tesque (Japan). For cytotoxicity testing and wound healing scratch assay, normal human dermal fibroblasts (NHDF) were purchased from Lonza (US). While, fetal bovine serum, Pierce™ Chromogenic Endotoxin Quant Kit, AlamarBlue® and Micro BCA™ Protein Assay Kit were from ThermoFisher Scientific, USA.

Hydrogel Formulation

LL37 Microspheres

Microspheres of LL37-loaded PLGA (50:50 MW 7,000–17,000 Da) were synthesized utilizing the water-in-oil-in-water (W/O/W) emulsion – solvent evaporation method [17]. Briefly, 20 mg of PLGA was dissolved in 1 mL of the dichloromethane. Twenty microgrammes of LL37 was dissolved in 20 µL of deionized water (DIW). The mixture was added to the PLGA solution, which was then sonicated at 70 W for 15 s in an ice bath to generate a W/O primary emulsion. The W/O/W emulsion was then formed by emulsifying the primary emulsion with 2 mL of 1% (w/v) polyvinyl alcohol (PVA, MW 13,000–23,000) dissolved in DIW, followed by sonication at 70 W for 15 s. This emulsion was added dropwise into 50 mL of 0.3% (w/v) PVA and stirred for 1 h at 600 rpm at room temperature to facilitate solvent evaporation. Subsequently, the resulting emulsion underwent three cycles of centrifugation at 22,000 × g, 4°C, for 40 min each, using DIW to eliminate any residual solvents such as PVA and dichloromethane and unencapsulated LL37. Blank MS, without LL37, were prepared using the same procedure. The MS were then subjected to lyophilization in a freeze-drier (Scanvac Coolsafe, France) for 24 h and stored at 4°C.

LL37 Microspheres Loaded in Activated Carbon-chitosan Hydrogel (LL37-AC-CS)

For the activated carbon-chitosan (AC-CS) hydrogel, 125 mg of CS powder and 0.1% (w/w) AC were mixed in 5 mL of distilled water to produce 2.5% (w/v) AC-CS hydrogel. The AC in CS solution underwent ultrasonication for 5 min at a frequency of 20 kHz and an amplitude of 40%. After mixing the solution on a magnetic stirrer for 1 h, 1% acetic acid was introduced to solubilize the CS. The resulting mixture was stirred for an additional 5 h. The procedure as described by Thoniyot et al. [18] was modified for the addition of PLGA MS to hydrogel [17]. To prepare LL37-AC-CS hydrogel, 15 mg MS were stirred in 5 mL AC-CS hydrogel using a magnetic stirrer for 30 min.

Physicochemical Characterisation

The particle size, PDI and zeta potential were determined from the lyophilised samples. One mL of sodium hydroxide (NaOH) 1 M was added to 15 mg LL37 MS, followed by sonication for 15 min and incubation at 37°C for 18 h with continuous shaking. The resulting mixture underwent neutralization with 1 M hydrochloric acid (HCl), followed

by centrifugation at 10,000 × g for 5 min. The supernatant was then subjected to analysis using the bicinchoninic acid (BCA) method, employing the Micro BCA™ Protein Assay Kit in accordance with the manufacturer's protocol. The encapsulation efficiency (EE) and drug loading capacity (DLC) were then calculated according to the following equations:

$$\text{Encapsulation efficiency, EE (\%)} = \frac{\text{Amount of LL37 in microsphere}}{\text{Total amount of LL37 in microsphere}} \times 100 \quad (1)$$

$$\text{Drug loading capacity, DLC (\%)} = \frac{\text{Amount of LL37 inmicrosphere}}{\text{Total amount of microsphere}} \times 100 \quad (2)$$

The particle size, zeta potential, and polydispersity index (PDI) of LL37 MS and blank MS were measured using Malvern Zetasizer Nano ZS (Malvern Instrument, UK) with refractive index 1.460, viscosity 0.8872 and DIW as dispersant at 25°C. The freeze-dried samples were diluted 1:10 with DIW and sonicated 1 min in an ice bath. The investigation involved the microscopic examination of the surface morphology of LL37 MS, CS, AC-CS, and LL37-AC-CS hydrogel in their freeze-dried states. This analysis was conducted utilizing a Field Emission Scanning Electron Microscope (FESEM) operating at 3 kV, with an average working distance ranging from 3.2 to 3.9 mm. Images were acquired at magnifications of 10,000 × and 25,000x.

In Vitro Drug Release Study

The drug release investigation utilized Transwell plate diffusion measurements with modification. Simulated wound fluid (SWF, pH 7.4) was as a dissolution medium of a Transwell plate (Corning, USA) [19]. LL37 MS, LL37 MS loaded in CS hydrogel, or LL37-AC-CS hydrogel were added into the Transwell insert lined with a semi-permeable membrane (porosity 0.4 µm). The SWF (w/w) was composed of 0.64% sodium chloride (NaCl), 0.22% potassium chloride (KCl), 2.5% sodium hydrogen carbonate ($NaHCO_3$), and 0.35% sodium dihydrogen phosphate (NaH_2PO_4) with the pH adjusted to 7.40. At predetermined time intervals, 0.5 mL of dissolution medium was taken. The *in vitro* drug release profile of LL37 was measured for 7 days by using Micro BCA™ Protein Assay Kit following the manufacturer's protocol.

LL37 Structural Integrity

In the assessment of microencapsulated protein integrity following *in vitro* release investigation, Sodium Dodecyl Sulfate–Polyacrylamide Gel Electrophoresis (SDS-PAGE) was conducted and compared with pure LL37 [19, 20]. The released peptides from the MS alone and hydrogel were obtained from the drug release study described in "In Vitro Drug Release Study" section. Briefly, 150 µL of the released media was aliquoted, and the protein content was quantified utilizing with the Micro BCA™ Protein Assay Kit. The peptide solution was then diluted 1:1 with Laemmli buffer and incubated for 5 min at 95°C. Ten microliter aliquots were loaded on 4% stacking and 16% resolving gel (Bio-Rad Laboratories, Germany; Mini-PROTEAN Tetra Cell) and ran at a constant voltage of 200 V (Power Pac 1000; Bio-Rad) in running buffer for 1 h. Post-electrophoresis, the gel was meticulously extracted, cleaned, stained with Coomassie dye for 1 h, destained via three water washes, and visualized using the GelDoc-IT Imaging System (Bio-Rad, USA).

Peptide-Polymer Interactions

The UV–Vis spectra of a pure LL37 solution in DIW and a solution specifically prepared for determining the EE of MS and released sample from LL37-AC-CS hydrogel were measured utilizing a UV–Vis spectrophotometer (Shimadzu 180, Japan) with a scan range set from 190 to 310 nm. Lyophilised LL37 MS, blank MS, formulated hydrogels such as CS, AC-CS and LL37-AC-CS hydrogels, and pure LL37, PLGA, AC, and CS powders were directly placed on the diamond attenuated total reflection (ATR) plate. Infrared spectra spanning the range of 4000–650 cm^{-1} were obtained using a Spectrum 400 FT-IR spectrometer (Perkin Elmer, USA) with 64 scans and a resolution of 4 cm^{-1} [21].

Bacterial Toxin Elimination Assay

The assessment of the interaction between the bacteria endotoxin and the LL37-AC-CS hydrogel was conducted employing a quantitative chromogenic Limulus Amebocyte Lysate (LAL)

and a Pierce™ Chromogenic Endotoxin Quant Kit. The absorbances endotoxins were measured at 405 nm using the NanoQuant Infinite M200 PRO microplate reader following the LAL incubation. In order to allow the MS to bind to the lipopolysaccharide (LPS), both LL37-AC-CS and blank MS loaded on AC-CS hydrogel were incubated with 1.0 EU of LPS in nonpyrogenic 96-well plates at 37°C for 30 min. After that, a total of 50 µL of this combination was added to an equivalent volume of LAL reagent (50 µL), and the mixture was further incubated for 10 min. Then, 100 µL of LAL chromogenic substrate was added to the mixture. The reaction was halted by adding 25% (v/v) glacial acetic acid, and the subsequent absorbance at 405 nm was determined after the release of p-nitroaniline [22].

In Vitro Cytotoxicity

The cytotoxicity of the hydrogel formulations to normal human dermal fibroblast (NHDF, ATCC® PCS-201–012™) cells was evaluated using AlamarBlue® assay. All hydrogels, neutralized and sterilized, underwent an overnight pre-soaking in cell culture medium. Subsequently, hydrogel leachates were collected after 24 h of incubation, and NHDFs were exposed to these leachates within the subsequent 24 h. The NHDF cells with passage number P3 were cultured in DMEM at a seeding density of 1×10^4 per well, supplemented with 10% FBS, 1% antibiotic (penicillin and streptomycin), and 90% DMEM. All cells were maintained at 37°C in a humidified atmosphere of 5% CO2/95% air. Hydrogel samples were washed with sterile Dulbecco's phosphate-buffered saline (DPBS), followed by a 24 h incubation in culture medium to obtain sterilized leachates through a 0.22 µm filter. Subsequently, the culture medium was replaced with 200 µL of hydrogel leachates per well, and the microplate was incubated for 24, 48, and 72 h. At the end of each time point, 10% AlamarBlue® was added to the fresh medium in each well and incubated for 4 h in the dark. Absorbance was measured on a spectrophotometer at 570 nm and 600 nm. Cell growth, indicative of toxicity, will be calculated using the following equation:

$$\% \text{ Reduction} = \frac{[(\varepsilon \text{ OX})\lambda 2A\lambda 1 - (\varepsilon \text{ OX})\lambda 1A\lambda 2]}{[(\varepsilon \text{ RED})\lambda 1A'\lambda 2 - (\varepsilon \text{RED})\lambda 2A'\lambda 1]} \times 100 \quad (3)$$

where $(\varepsilon OX)\lambda 2 = 117{,}216$; $(\varepsilon OX)\lambda 1 = 80{,}586$; $(\varepsilon RED)\lambda 1 = 155{,}677$; $(\varepsilon RED)\lambda 2 = 14{,}652$; $A\lambda 1$ and $A\lambda 2$ = observed absorbance reading for test well at 570 and 600 nm, respectively; A' λ1 and A' λ2 = observed absorbance reading for negative control well at 570 and 600 nm, respectively.

In Vitro Wound Healing Scratch Assay

The wound healing scratch assay was conducted with slight modifications based on the procedure established by Liang et al. [23]. A lower percentage of fetal bovine serum (5%) was used in the growth medium (10%) to reduce the amount of cell proliferation while maintaining an adequate level to prevent apoptosis and/or cell detachment. The NHDF cells were grown to 80–90% confluence, were seeded at a density of 3×10^5 cells per mL in a 24-well plate. Each well in the 24-well plate was allocated a loading volume of 500 µL. After the seeding was complete, the plates were incubated for 24 h at 37°C and in an environment containing 5% carbon dioxide. A sterile pipette tip was employed to create a scratch in the monolayer of confluent cells at the center of each well. After that, three separate washings using DPBS solutions were performed to remove cell debris from the scratches. The inverted microscope that comes with the digital microscopic camera was used to take images of the scratches in each well at 0, 24, 48, and 72 h after the scratching began at the same location at each time point.

Antimicrobial and Antibiofilm Activities

Minimum Inhibitory Concentrations (MIC)

Polypropylene microtiter plates were employed, in lieu of traditional 96-well plates, to mitigate undesired nonspecific binding of peptides to the plate walls. Briefly, *S. aureus* (ATCC 25923), *E. coli* (ATCC 25922), and *P. aeruginosa* (ATCC 27853) were cultured in Mueller Hinton broth (MHB) for a 24-h cycle. A 20-fold concentrated stock solution was prepared, and serial dilutions of the AMPs were executed on 96-well polypropylene microtiter plates containing MHB, supplemented with 0.4% bovine serum albumin and 0.2% acetic acid. Each well, containing 100 µL of MHB, was inoculated with 5×10^5 CFU/mL of the respective bacteria, along with varying concentrations of LL37 (ranging from 0.125 µg/mL to 64 µg/mL).

The broth micro-dilution method was employed to ascertain the MIC of LL37-AC-CS hydrogel against *S. aureus*, *E. coli*, and *P. aeruginosa*. A sterile 96-well microplate with a flat bottom was utilized to prepare a dilution series of LL37-AC-CS and AC-CS hydrogels in MHB, ranging from 500 mg/mL to 0.976 mg/mL. Bacterial inoculum was created by introducing a single, pure colony of cultured bacteria into 10 mL of MHB, followed by incubation at 37°C for 24 h. Turbidity adjustment of the microorganisms was achieved using a spectrophotometer, measuring absorbance at 600 nm within the range of 0.08 to 0.125. Subsequently, the bacterial inoculum was diluted with MHB and further diluted at a 1:100 ratio. A 100 µL volume of the resulting bacterial solution was added to each well, with negative controls consisting of solely bacterially strained MHB. The microplate was then incubated at 37°C overnight. Post-incubation, 10

µL aliquots were extracted from the wells to assess bactericidal activity. These aliquots were spread on MHA in petri dishes and incubated at 37°C overnight, followed by recording of resulting growth. Staining of the wells was accomplished using 20 µL of 2,3,5-triphenyltetrazolium chloride (TTC) reagent (0.2% w/v). TTC serves as an indicator, being reduced to red formazan in the presence of bacteria, indicating bacterial activity and viability.

Additionally, bactericidal activity against *S. aureus, E. coli,* and *P. aeruginosa* was ascertained employing the broth micro-dilution method with released samples as a previous study with slight modification [24]. From the Transwell drug release experiment, the antibacterial capabilities of AC-CS hydrogel containing LL37 MS were carried out. Transwell drug release into the dissolution medium was sampled at 6, 12 and 24 h and was quantified with a BCA kit prior to antimicrobial assay using the broth micro-dilution method as described above.

***In Vitro* Antibiofilm Properties** The 2,3-bis(2-methoxy-4-nitro-5-sulfophenyl)-2H-tetrazolium-5-carboxanilide (XTT) colorimetric experiment was carried out in a 96-well polystyrene plate to examine the effect that the LL37-AC-CS hydrogel had on preventing the formation of biofilm. Dilutions of LL37-AC-CS and AC-CS hydrogels, ranging from 500 mg/mL to 0.976 mg/mL, were prepared in MHB using a sterile flat-bottomed 96-well microplate. *S. aureus*, *E. coli*, and *P. aeruginosa* bacteria were cultured in MHB at 37°C for 24 h, and their turbidity was adjusted spectrophotometrically. To ensure proper adhesion of biofilm to well walls, 100 µL of bacterial solution was pipetted into each well using a multichannel pipette, followed by a 24-h incubation period. Subsequently, planktonic cells and media components were removed by inverting the plate, and the remaining planktonic bacteria were rinsed three times with pre-warmed sterile phosphate-buffered saline (PBS). After discarding cells and samples, the wells were washed with sterile PBS. Following these preparations, 100 µL of sterile PBS and 100 µL of XTT-menadione solution were added to the treatment well. The mixture was incubated for 4 h at 37°C in the dark.

Additionally, cells adhered to wells were subjected to treatment with 100 µL samples derived from the dissolution media of the Transwell drug release experiment. Concentrations were prepared from collected fluid at 6, 12, and 24 h, followed by measurement using a BCA kit. For the biofilm experiment, wells were treated with each concentration, while non-treated cells were incubated with 100 µL of PBS, and the plates were subsequently incubated for 24 h at 37°C. The percentage of biofilm formation inhibition was determined using the following equation:

$$\%\ \text{biofilm inhibition} = \frac{\textit{Absorbance of}\ \text{blank control} - \text{Absorbance of test sample}}{\textit{Absorbance of}\ \text{blank}\ \textit{control}} \times 100 \quad (4)$$

In Vivo* Biofilm Formation in *C. Elegans The antibiofilm efficacy of LL37 against biofilms formed by *S. aureus*, *E. coli,* and *P. aeruginosa* was assessed using the nematode *Caenorhabditis elegans* (*C. elegans*) following a methodology adapted from Ali et al. [25]. Bacterial cultures in MHB were maintained in a 37°C incubator for 24 h. After eliminating planktonic bacteria, the adherent biofilm on the wall was allowed to mature in MHB for an additional 24 h. Subsequently, the concentration of bacterial biofilm suspensions was adjusted to the 0.5 McFarland standard, and 100 µl was inoculated into microcentrifuge tubes. Each tube received a group of 25 L4 larval stage worms, 1 mL of M9 buffer, and LL37 MS within a hydrogel matrix. Worms were maintained at 20°C for 24 h. A control group of worms was exposed to bacterial biofilm in MHB alone. Post-incubation, worms underwent three washes with sterile M9 buffer and 0.1 M sodium azide. Following staining with 1 mg/mL acridine orange for three minutes in each bacterial batch, the bacteria were thrice washed with M9 buffer. Confocal laser scanning microscopy (CLSM, A1R Nikon, USA) at 20× magnification was employed to visualize the worms, and the extent of biofilm colonization within the *C. elegans* gastrointestinal tract was assessed by measuring intensity profiles emitted from their bodies.

Statistical Analysis All data were expressed as the mean ± standard deviation. Statistical analysis was conducted through one-way ANOVA using Graph Pad Prism 9, accompanied by Tukey's post hoc test for multiple comparisons. Significance levels were established at $p < 0.05$, denoting statistical significance among the groups under examination. The measurements were conducted in triplicate, and the results are reported as the mean value accompanied by the standard deviation (SD).

Results and Discussion

Characterization of Microspheres and Hydrogels

LL37 MS were synthesized using the double (water-in-oil-in-water) emulsion solvent evaporation method, employing polyvinyl alcohol (PVA) as a stabilizing agent. The size, PDI, zeta potential, and encapsulation efficiency of LL37 MS and blank MS are presented in Table I. The results found here are in parallel with previous studies [17, 26]. Encapsulation efficiency was greater than 80%, which is economically advantageous for the formulation of peptides.

Table I Properties of LL37 Microspheres and Blank Microspheres (Mean ± SD, $n = 3$)

Name	Particle size (nm)	PDI	Zeta potential (mV)	Encapsulation efficiency (%)	Drug loading capacity (%)
LL37 microspheres	302.37 ± 5.23	0.081 ± 0.006	-23.1 ± 1.07	84.25 ± 3.98	0.112 ± 0.0513
Blank microspheres	297.43 ± 2.33	0.070 ± 0.020	-20.5 ± 1.29	-	-

Encapsulation efficiency is an important parameter in the development of peptide-based formulations because it directly affects the efficacy and stability of the formulation. Peptides are fragile molecules that are prone to degradation, denaturation, and aggregation, which can compromise their biological activity and therapeutic potential [27, 28].

LL37 is a cationic antimicrobial peptide. Studies have shown that the presence of alginate, an anionic polymer, induces a change in the helical structure of LL37, thereby impacting its antimicrobial effects [29, 30]. As a result, a promising alternative for hydrogel formulation is the utilization of a cationic polymer, such as chitosan (CS). The method employed for the formation of the composite involves physical embedding [17, 18]. This suggests that LL37 microspheres are physically incorporated or dispersed within the AC-CS hydrogel matrix. The physical interactions between the components could include van der Waals forces, hydrogen bonding, or other non-covalent interactions [31, 32].

Figure 1a and b shows the CS hydrogel and after the addition of AC, respectively. The incorporation of AC significantly enhanced the smoothness and network properties of the composite, potentially due to the π bonding interaction between carbon and the amino/hydroxyl groups of CS [33]. A uniformed dispersion of AC is achieved within the CS matrix, mitigating any concerns of agglomeration [34]. The incorporation of AC into CS hydrogels was shown to enhance the structural integrity and networking of the CS hydrogel. The extensive surface area of AC can enhance the interfacial adhesion between CS and carbon particles, thereby increasing the mechanical strength and elasticity of the resulting hydrogel [35, 36]. From Fig. 1c, the LL37 MS appeared spherical with tiny bumps on their surfaces. LL37 MS were well-distributed and embedded in the formulated hydrogel (Fig. 1d). This suggests that the MS were evenly dispersed throughout the hydrogel matrix and were not clumped together in a particular area. This is important because it ensures that the therapeutic agent (LL37) encapsulated within the MS is evenly distributed throughout the hydrogel.

In Vitro Drug Release

The release studies are conducted to understand the controlled release of therapeutic agents from drug delivery systems, such as gels or other formulations. The duration of release studies can vary and may not necessarily match the entire healing process of a critical wound. Generally, Transwell membranes with smaller pore sizes (0.4 or 3 µm) are predominantly employed in drug transport studies as recommended by the manufacturer's manual (Corning, USA). The selection of the specific 0.4 µm porosity for the Transwell membrane was also based on the methodology outlined by Puvirajesinghe et al. [19]. The chosen membrane porosity mimics the physiological barriers encountered *in vivo* and allows to assess release kinetics under conditions that simulate physiological barriers. Thus, the decision to opt for a 0.4-micron pore size aims to facilitate the passage of smaller molecules, such as LL37, while concurrently impeding the movement of larger molecules or particles within the hydrogel system.

The drug release results (Fig. 2a) revealed that LL37 MS have a significantly higher peptide release rate than LL37 MS loaded on the formulated hydrogel. This outcome is consistent with a previous study involving platelet-derived growth factor receptor (PDGF) released from PLGA MS embedded in CS hydrogel [37] and platelet lysate-loaded PLGA nanoparticles (NP) in Pluronic F-127 hydrogel intended for wound treatment [38]. LL37 MS and MS entrapped within hydrogels typically followed a biphasic pattern with zero-order kinetics, characterised by an initial rapid release followed by a more gradual sustained release [17]. In the first 24 h, the MS exhibited a notable initial release of 21.08%. The burst release in hydrogels formulated with CS and AC-CS containing the MS was slightly delayed, measuring 19.33% and 18.15%, respectively. However, this delay was not statistically significant when compared to MS containing LL37. By the seventh day (168^{th} h), significantly more LL37 had been released from the MS (88.42%), compared to MS in CS (72.39%) and AC-CS hydrogel (70.18%). The amount of drug released from PLGA MS is regulated by both drug diffusion and polymer erosion. Additionally, because PLGA absorbs water, polymer breakdown occurs within the bulk of the particle and on its surface, known as "bulk erosion" and "surface erosion," respectively. To achieve a consistent release over time, it is essential for the interplay between diffusion and erosion processes to be in equilibrium, ensuring a steady rate of peptide diffusion from the MS [39].

Interestingly, there were no significant differences ($p > 0.05$) between the rate drug release profiles of LL37 MS loaded on CS and AC-CS hydrogel, suggesting that the AC in AC-CS hydrogel may have a weak or no effect on MS drug release. The study found that higher AC concentration in the scaffold leads to a slower release of the drug due to the porous scaffold

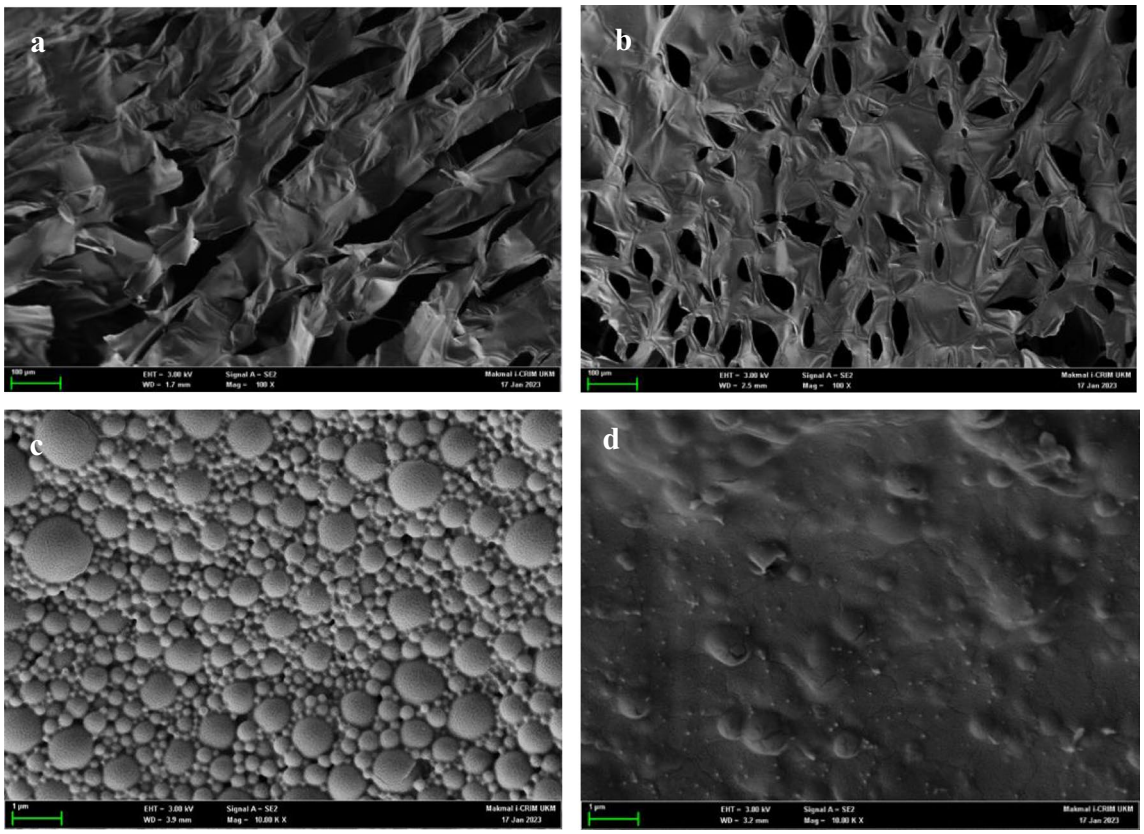

Fig. 1 FESEM images of CS hydrogel (**a**) and AC-CS hydrogel (**b**) at magnification of 100x. LL37 microspheres (**c**) and LL37-AC-CS hydrogel (**d**) images are at magnification of 10,000x

that may act as traps for the drug. This facilitates a gradual and long-lasting healing process, while samples with lower AC concentration released the drug more rapidly due to their reduced adsorption capacity. It is worth noting that the scaffold with the highest AC concentration released 40% of the drug in the initial 3 h, subsequently maintaining a gradual release, effectively minimizing the risk of bacterial infection in the vicinity of the implant [40]. Hydrogel formulated for sustained release is also beneficial for long term chronic wound healing.

Stability of LL37

LL37 Structural Integrity

The preparation process for MS may affect the integrity of the proteins they carry. The harsh conditions, including organic solvents, high temperatures, and mechanical agitation, have the potential to cause irreversible denaturation of the proteins, leading to the loss of protein function. Figure 2b revealed that the characteristic bands of LL37 were present and in the same position across all groups. This finding suggests that the molecular weight and structural integrity of LL37 were likely unaffected by the W/O/W method employed for MS preparation and their incorporation into the hydrogel formulation.

Peptide-Polymer Interactions

UV–Vis spectroscopy was employed to assess the compatibility of LL37 within the MS, EE, and the released samples. The results showed that there was no drug-polymer interaction, and the structural integrity was maintained after formulated in MS and hydrogel, as evidenced by the identical UV spectra observed in pure LL37, EE (Fig. 2c), and released samples (Fig. 2d).

FTIR analysis was performed to examine the interaction between drugs and polymers. LL37 MS was found to display a slight shift in the amide I peak of the α-helical peptide LL37, which typically occurs at 1652 cm^{-1} but was observed at 1647 cm^{-1} [41, 42]. However, the amide II peak remained at 1541 cm^{-1} in pure LL37 and after encapsulated in PLGA MS. The pure PLGA 50:50 exhibited characteristic peaks, including OH stretching (3200–3500 cm^{-1}), –CH (2850–3000 cm^{-1}), carbonyl –C = O stretching (1700–1850 cm^{-1}), and C–O stretching (1050–1250 cm^{-1}). The peaks at 1748 cm^{-1}

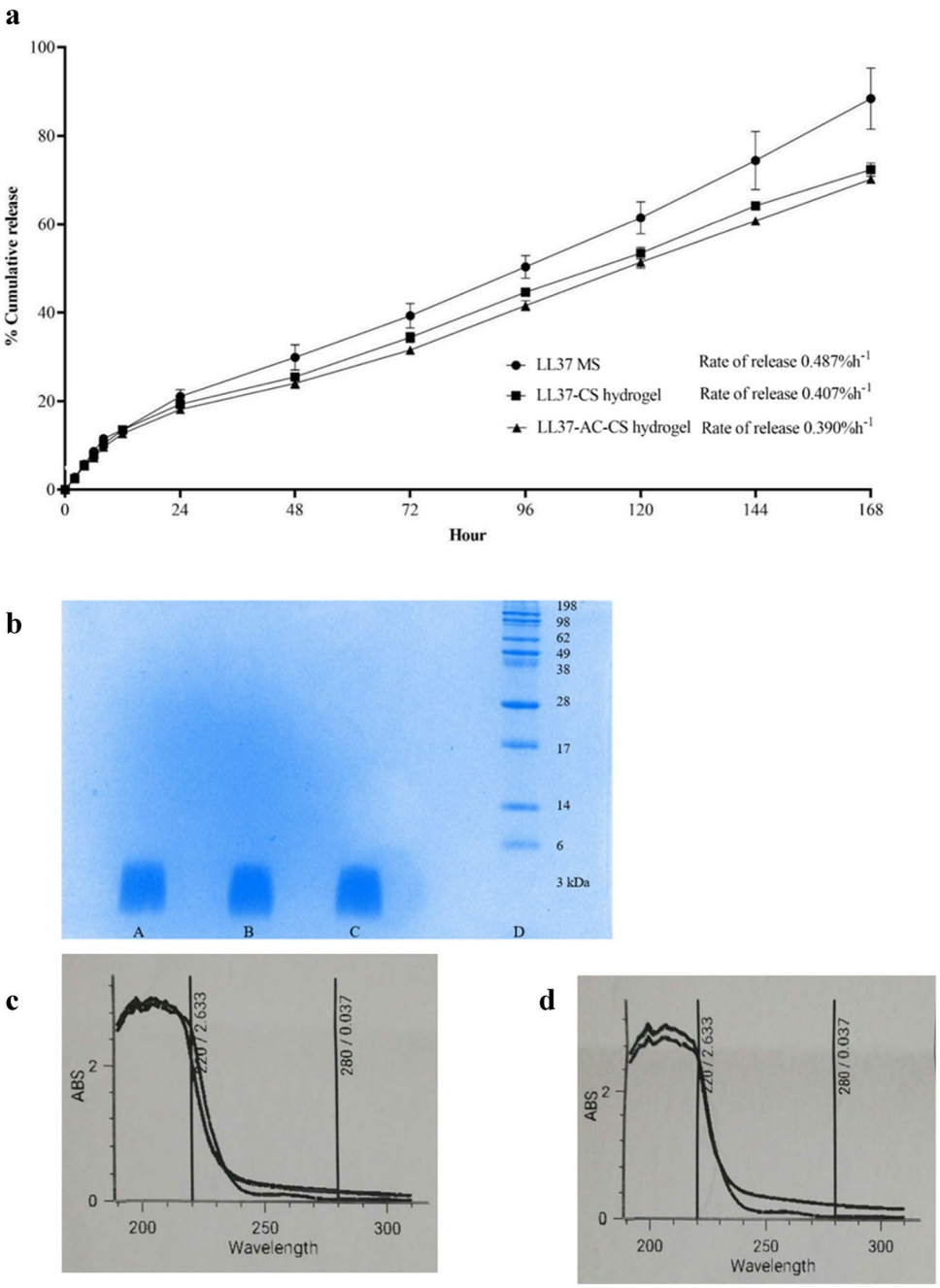

Fig. 2 **a** *In vitro* release of LL37 (plotted as a function of % cumulative release vs time) from LL37 microspheres, LL37-CS hydrogel and LL37-AC-CS hydrogel (mean ± SD, $n = 3$). **b** SDS-PAGE analysis of (A) original LL37, (B) LL37 released samples from microspheres, (C) LL37 released samples from microspheres in hydrogel and (D) protein ladder. UV–Vis spectra of **c** pure LL37 with EE sample and **d** pure LL37 with released samples from LL37-AC-CS hydrogel

and 1166 cm^{-1} corresponded to the carbonyl -C = O and C-O stretching bands of ester groups of L-lactide and glycolide units in PLGA, respectively. However, upon comparing the LL37 MS with blank MS, it was noted that the absorption bands of both LL37 and PLGA were evident in the former, with no chemical shift observed, thus indicating that the encapsulation of LL37 was successful without any chemical interaction between the MS compounds as depicted in Fig. 3a. This outcome aligns with a prior investigation [38].

From Fig. 3b, the FTIR analysis indicates that the AC has abundance of functional groups, implying the presence of adsorption sites on its surface. The observed peaks at 3440 cm^{-1} correspond to the vibration of the –OH bond, 2940 cm^{-1} are due to C–H stretching and 1740 corresponds to the C = O group. The existence of these functional groups enhances the adsorption ability of the AC [43]. CS exhibited a wide band ranging from 3500–3000 cm^{-1}, attributed to the stretching vibrations of OH and NH functional groups involved in hydrogen bonding. The characteristic absorption bands observed at 1647 cm^{-1} were indicative of the C = O

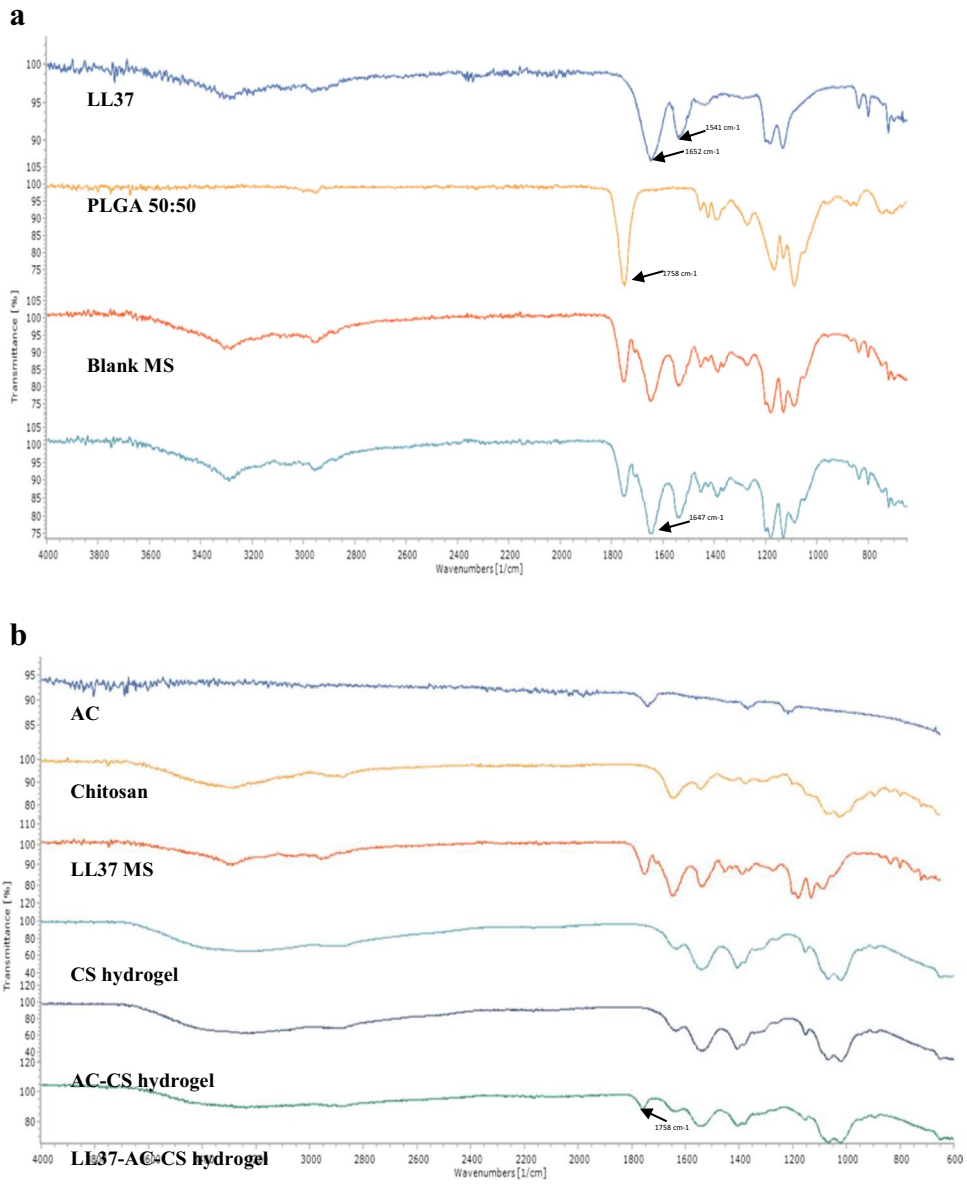

Fig. 3 **a** FTIR spectra of pure LL37, PLGA 50:50, LL37 MS and blank MS **b** FTIR spectra of pure AC, chitosan, LL37 MS, CS hydrogel, AC-CS hydrogel LL37-AC-CS hydrogel

stretching in the amide I vibration, while the absorption band detected at 1542 cm-1 was attributed to the N–H bending in the amide II vibration and 1375 cm^{-1} for C-N stretching of amide III. Notably, there were no significant difference peaks observed between the CS hydrogel and the AC-CS hydrogel. It is worth noting that the hydrogel containing AC did not display any additional peaks, which implies that AC might not have an impact on the physical and chemical interactions occurring within the hydrogel. The absence of a distinct AC characteristic peak in the AC-CS hydrogel could be attributed to the relatively lower concentration of AC in comparison to CS within the composites. However, when comparing LL37-AC-CS hydrogel with CS and AC-CS hydrogels, an additional peak emerged at 1758 cm^{-1}, corresponding to the carbonyl group (C = O) stretching vibration of the ester bond in PLGA [38]. This indicates that PLGA MS encapsulated with LL37 was successfully fabricated on the AC-CS hydrogel (Fig. 3b).

Bacterial Toxin Elimination Assay

It is hypothesised that antimicrobial wound dressing which eliminates bacteria toxins can accelerate wound healing. Incorporation of AC into the wound dressing formulation is a plausible strategy as AC is a high porosity biomaterial and known for their toxin removal properties. The effect of LL37-AC-CS hydrogel on LPS endotoxin removal was examined using a chromogenic quantitative LAL assay. From the results, the LL37-AC-CS hydrogel (73.13%) bound a

significantly greater percentage of endotoxin than blank MS loaded on AC-CS hydrogel only (62.54%). In addition to AC, LL37 could also bind to and neutralises LPS endotoxin at concentrations greater than 1 µg/mL or 0.2 µM [44, 45]. Another study also showed that an antimicrobial dressing incorporating AC demonstrates the capacity to adsorb bacteria, exotoxins, and endotoxins, thereby expediting the healing process in chronic wounds [46]. An *in vitro* study has shown

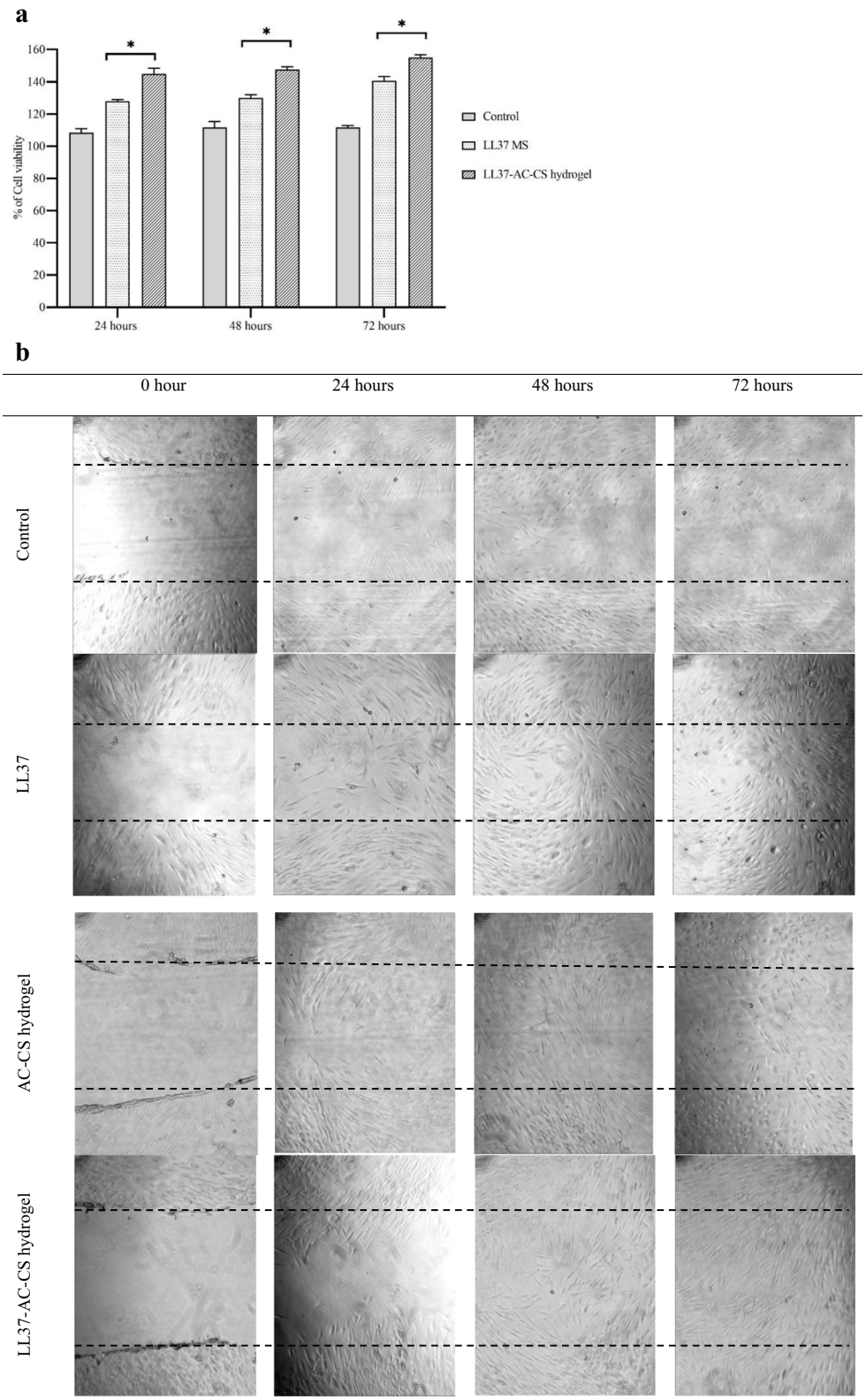

Fig. 4 **a** The percentage of cell viability using the AlamarBlue® assay at 24, 48 and 72 h. The asterisks (*) represent significant difference ($p < 0.05$, respectively) compared to control. **b** Migration of NHDFs treated with hydrogels for 24, 48, and 72 h. **c** Wound gap area closure at different time points; expressed in mean ± SD, $n = 3$. The * represent statistically significant difference ($p < 0.05$) compared to control. **d** Bacterial growth of Transwell released sample on TTC and MHA

Fig. 4 (continued)

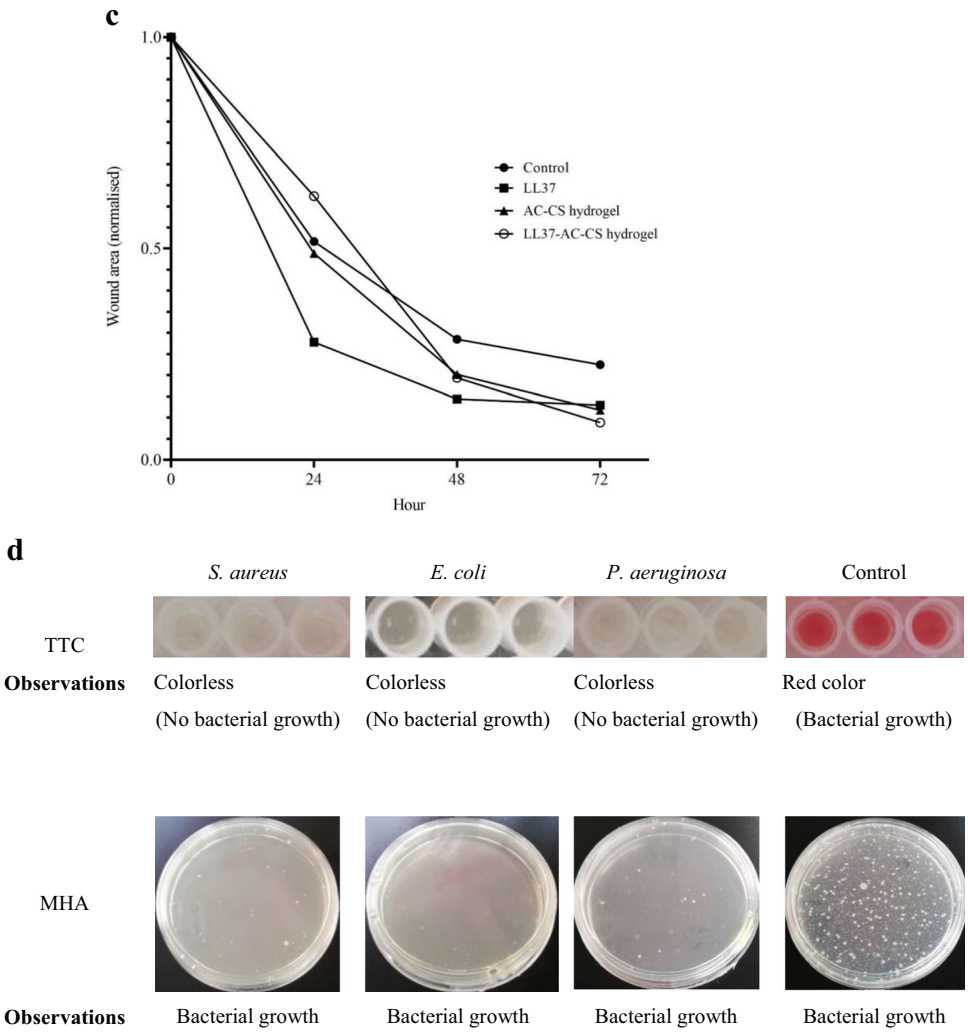

the efficacy of an AC dressing with silver, in selectively binding to LPS without the concomitant release of *P. aeruginosa* endotoxins into the surrounding environment [47].

In Vitro Cytotoxicity

Fibroblast skin cells, essential for the natural wound-healing process, are commonly employed in *in vitro* cytotoxicity assessments of hydrogels, as they directly interact with wound dressings. The AlamarBlue® assay was utilised to determine if the hydrogel was cytotoxic to NHDF cells, in comparison to the control. After treatment, all the cells exhibited signs of viability and proliferation, particularly the LL37-AC-CS hydrogel after 24, 48, and 72 h of treatment (Fig. 4a). This study found that the incorporation of AC stimulated cell proliferation, potentially because the AC contained hydrophilic functional groups that improved protein adsorption and facilitated cellular attachment onto the composite scaffolds. LL37 has demonstrated a critical role in the wound healing process by inducing fibroblast proliferation at concentrations of 1 to 5 µM [48, 49]. The prepared hydrogel may have a synergistic proliferation

Table II MIC and MBC of LL37, Gentamicin, LL37-AC-CS Hydrogel, and AC-CS Hydrogel Against Bacteria

Bacteria	LL37		Gentamicin		LL37-AC-CS hydrogel		AC-CS hydrogel	
	MIC (µg/mL)	MBC (µg/mL)	MIC (µg/mL)	MBC (µg/mL)	MIC (mg/mL)	MBC (mg/mL)	MIC (mg/mL)	MBC (mg/mL)
E. coli	2	4	2	2	62.5	125	125	250
P. aeruginosa	16	16	0.5	0.5	31.25	62.5	125	250
S. aureus	4	8	0.5	0.5	31.35	62.5	62.5	125

effect with the CS. The promotion of fibroblast proliferation was significantly pronounced with CS characterised by elevated degrees of deacetylation [50]. The excellent viability (> 80%) observed in the LL37-AC-CS hydrogel with NHDFs indicates their promising use as wound dressings.

In vitro Wound Healing Assay

The impact of the formulations on NHDF migration was evaluated using an *in vitro* wound healing scratch assay over a period of 24, 48, and 72 h (Fig. 4b). In Fig. 4c, three treatment groups were found statistically significant differences ($p < 0.05$) across all the time points in comparison to the control. However, when compared to LL37-AC-CS hydrogel, LL37 alone demonstrated much faster levels of cell migration at 24 and 48 h. This could be due to the slow release of the LL37 from the MS entrapped within the hydrogel. However, LL37-AC-CS hydrogel demonstrated the highest wound closure at 72 h among groups. This demonstrated that LL37 retained its biological activity when incorporated into a PLGA MS system with AC-CS hydrogel. LL37 has been demonstrated as a crucial element in the wound healing mechanism by stimulating fibroblast migration at a concentration as low as 1 µM, as reported by Oudhoff et al. in 2010 [49].

In Vitro Antimicrobial Activity

Direct Treatment

The obtained MIC values for LL37 were 2, 4, and 16 µg/mL for *E. coli*, *S. aureus*, and *P. aeruginosa*, respectively. The MIC and MBC were similar for *P. aeruginosa* but higher for *E. coli* (4 µg/mL) and *S. aureus* (8 µg/mL) (Table II). The LL37-AC-CS hydrogel demonstrated MIC values of 62.5 mg/mL for *E. coli* and 31.25 mg/mL for *S. aureus* and *P. aeruginosa*, while the MBC values for all three bacteria were higher, at 125 mg/mL for *E. coli* and 62.5 mg/mL for both *S. aureus* and *P. aeruginosa*. However, as shown in Table II, the AC-CS hydrogel required a higher concentration compared to LL37-AC-CS hydrogel to effectively inhibit bacterial growth. This indicates that the LL37 was released from the hydrogel of LL37 MS, thereby demonstrating its antimicrobial effect against all three types of bacteria.

Treatment with Released Sample

After quantification using a BCA protein kit, the LL37 released from Transwell at 6, 12, and 24 h were found to be 1.51, 2.25, and 3.17 µg/mL, respectively. Interestingly, none of the three bacteria (*S. aureus, E. coli, and P. aeruginosa*)

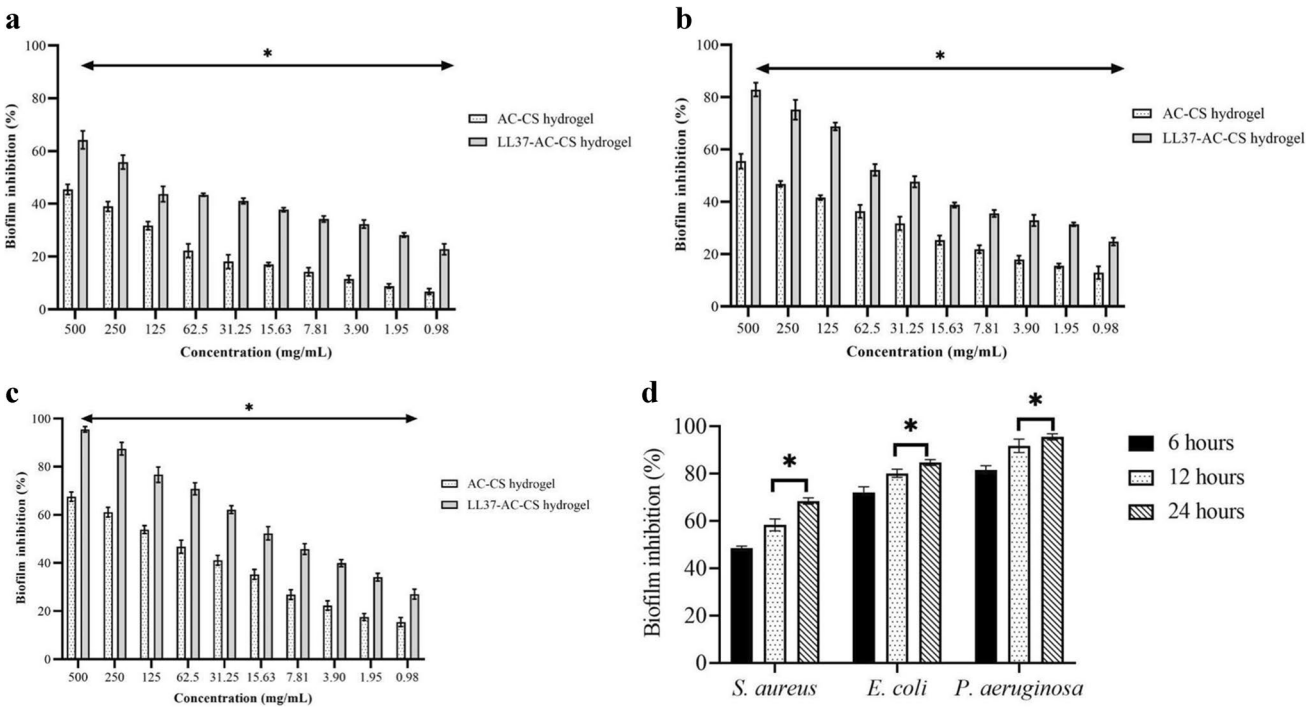

Fig. 5 The percentage of biofilm inhibition at different concentration of AC-CS and LL37-AC-CS hydrogels for **a** *S. aureus*, **b** *E. coli* and **c** *P. aeruginosa*. The * represent statistically significant difference ($p < 0.05$) compared to AC-CS hydrogel. **d** The percentage of biofilm inhibition for 6, 12 and 24 h released sample for *S. aureus*, *E. coli* and *P. aeruginosa*. Mean concentrations of released samples were 1.32, 2.03, and 3.03 µg/mL at 6, 12, and 24 h, respectively. The * represent statistically significant difference ($p < 0.05$) compared to 6 h

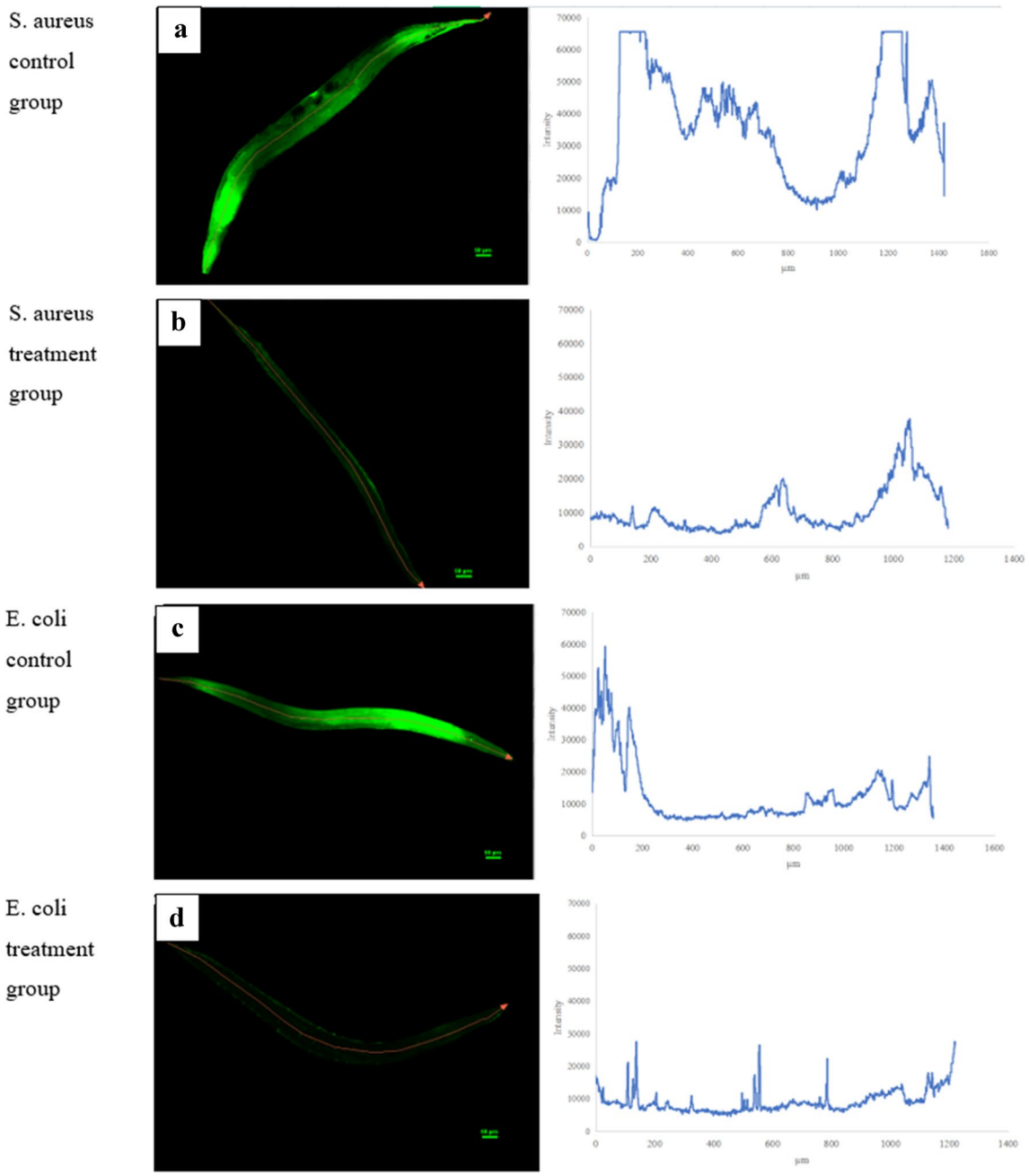

Fig. 6 Fluorescence intensities profile of *C. elegans* infected with *S. aureus*, *E. coli* and *P. aeruginosa* by CLSM. **a**, **c** and **e** were control group while **b**, **d** and **f** were treated with LL37-AC-CS hydrogel

demonstrated visible growth (i.e., no formation of red colour) after being treated with TTC. However, when 10 µL aliquots were taken from the wells to determine bactericidal activity, all resulted in bacterial growth following overnight incubation at 37°C (Fig. 4d). The released samples of the formulated hydrogels exhibited lower concentrations required for bacterial growth, which may be attributed to the synergistic antimicrobial effect of the CS hydrogel. As a cationic peptide (+ 6), LL37 exerts its bactericidal effect by binding to the negatively charged bacterial membrane, inducing cell lysis and promoting cell death through membrane disruption [51, 52]. It is noteworthy that CS, possessing inherent antimicrobial properties, acts through electrostatic interactions with microbial cell membranes, leading to membrane interruption and subsequent cell death [53]. Overall, LL37 and CS act as a promising combination for the formulation of antimicrobial dressing, with the potential for enhanced efficacy when integrated with porous materials such as AC.

In Vitro Antibiofilm Activity

XTT is a tetrazolium salt and this method measures the reduction of water-soluble formazan in viable cells, and the absorbance measurement can be directly read, making the procedure efficient and intuitive. LL37 and CS inhibited the formation of biofilm in a dose-dependent manner. For direct treatment, the LL37-AC-CS hydrogel exhibited significantly higher biofilm inhibition than the AC-CS hydrogel as shown by the XTT assay results for *S. aureus* (Fig. 5a), *E. coli* (Fig. 5b), and *P. aeruginosa* (Fig. 5c). Notably, the LL37-AC-CS hydrogel demonstrated the greatest biofilm inhibition for *P. aeruginosa*, followed by *E. coli* and *S. aureus*.

Following the quantification with the BCA kit, the released samples exhibited mean concentrations of 1.32, 2.03, and 3.03 µg/mL at 6, 12, and 24 h, respectively. As depicted in Fig. 5d, the formulated hydrogel demonstrated superior inhibition of biofilm formation by *E. coli* and *P. aeruginosa* compared to *S. aureus* due to electrostatic interaction with bacterial membranes. Previous research has shown that Gram-negative bacteria attach more strongly to AC and are harder to wash away than Gram-positive bacteria [54]. *In vitro*, LL37 was able to prevent the biofilm formation caused by *S. aureus*, *E. coli,* and *P. aeruginosa* at significantly lower concentrations than those required for inhibiting bacterial growth or inducing bacterial lethality, while preserving bacterial viability [55].

LL37 released from LL37-AC-CS hydrogels has shown promising results in combating biofilm growth and development in bacteria by targeting them at various stages. LL37 can obstruct cell attachment and disrupt pre-formed and mature biofilms [56]. Kang et al. (2019) found that LL37 exhibits superior anti-biofilm activity against *S. aureus* biofilms compared to silver nanoparticles and traditional antibiotics [57]. Notably, LL37 exhibited pronounced effectiveness in inhibiting the formation of *P. aeruginosa* biofilms *in vitro*, even at a notably diminished and physiologically relevant concentration of 0.5 µg/mL, a concentration significantly below the MIC, as reported by Joerg et al. [58]. It is noteworthy, however, that a higher concentration of LL37 was needed to prevent biofilm formation in *S. aureus*. Furthermore, LL37, even at low concentrations, demonstrated the capacity to impede biofilm formation by *E. coli* [59].

Biofilm Formation in *C. Elegans*

Earlier research using the *C. elegans* model revealed that bacteria form biofilm inside the intestinal tract of the worms [60]. To further evaluate the effectiveness of LL37-AC-CS hydrogel against biofilm formation, we conducted an *in vivo* experiment on *C. elegans* worms, comparing the fluorescence intensity profiles of treated and untreated worms infected with *S. aureus*, *P. aeruginosa*, and *E. coli* biofilms. A robust positive correlation was evident between the number of biofilm

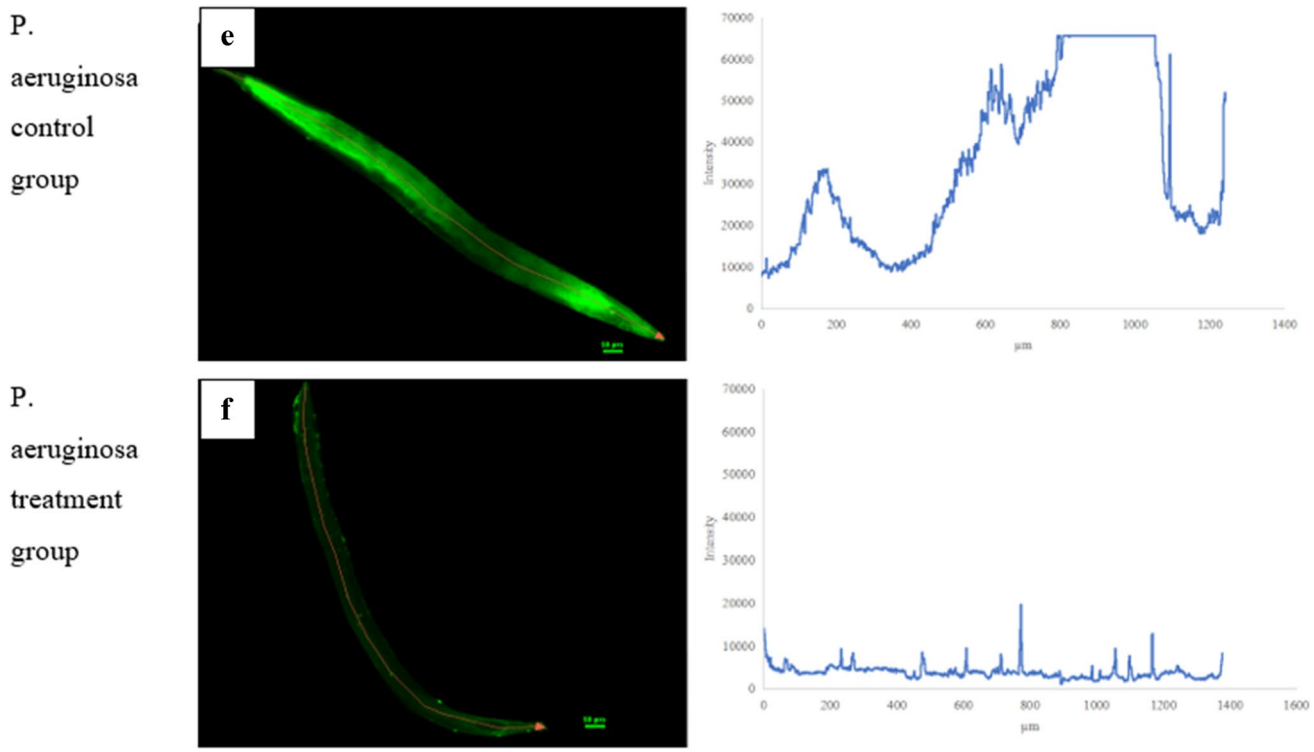

Fig. 6 (continued)

bacteria that had colonised the worms and the emitted light intensity. The results, depicted in Fig. 6, showed that control worms had higher intensities than those treated with the formulated hydrogel, indicating the presence of bacterial colonization in the nematode intestine. This suggests that the antibiofilm action is effective against all three bacteria *in vivo*. Moreover, when *C. elegans* were exposed to treated *P. aeruginosa* and *E. coli*, the decrease in fluorescence intensity was more noticeable than in *S. aureus*, indicating the capability of LL37-AC-CS hydrogel in inhibiting biofilm formation, especially in Gram-negative bacteria. The *in vivo* results align with those obtained from the *in vitro* XTT assay.

Conclusions

The study has successfully formulated and characterized LL37 MS loaded on AC-CS hydrogel, and the hydrogel has demonstrated to possess antimicrobial and antitoxin properties. The MS have successfully encapsulated and protect LL37 from the method of preparation. The biphasic release pattern of the MS provides a high initial release followed by a sustained release, which is beneficial for long-term wound healing such as chronic wounds. The LL37-AC-CS hydrogel also demonstrated antibiofilm activity and the AC can effectively adsorb bacterial endotoxins. In conclusion, LL37-AC-CS hydrogel is stable, non-toxic, with enhanced antimicrobial and antitoxin activity, and can be potentially applied to chronic wound infections to accelerate wound healing. This research has warranted an *in vivo* study to determine its safety and efficacy in wound healing.

Acknowledgements Authors would like to thank the Faculty of Pharmacy, UKM for the research facilities support and special thanks to UKM Medical Molecular Biology Institute (UMBI) for supporting the C. elegans work.

Authors' Contributions Conceptualization and methodology, S.-F. Ng., writing—original draft preparation, B.-Y. Lim., and S.-F. Ng.; review and editing, F.Azmi. and S.-F.Ng. funding acquisition, S.-F. Ng. All authors have read and agreed to the published version of the manuscript.

Funding This research is financially supported by the research grant no. GUP-2019–003, Universiti Kebangsaan Malaysia (UKM).

Data Availability The raw data presented in this study are available on request from the corresponding author.

Declarations

The authors declare that they have no known competing financial interests or personal relationships that could have appeared to influence the work reported in this paper.

Ethics Approval and Consent to Participate Not applicable.

Consent for Publication Not applicable.

Competing Interests None.

References

1. Sen CK. Human wound and its burden: Updated 2020 compendium of estimates. Adv Wound Care (New Rochelle). 2021;10:281. https://doi.org/10.1089/WOUND.2021.0026.
2. Sanya DRA, Onésime D, Vizzarro G, Jacquier N. Recent advances in therapeutic targets identification and development of treatment strategies towards Pseudomonas aeruginosa infections. BMC Microbiol. 2023;23:86. https://doi.org/10.1186/s12866-023-02832-x.
3. Paleczny J, Junka A, Brożyna M, Dydak K, Oleksy-Wawrzyniak M, Ciecholewska-Juśko D, Dziedzic E, Bartoszewicz M. The high impact of staphylococcus aureus biofilm culture medium on in vitro outcomes of antimicrobial activity of wound antiseptics and antibiotic. Pathogens. 2021;10:1387. https://doi.org/10.3390/PATHOGENS10111385/S1.
4. Frykberg RG, Banks J. Challenges in the treatment of chronic wounds. Adv Wound Care (New Rochelle). 2015;4:560. https://doi.org/10.1089/WOUND.2015.0635.
5. Omar A, Wright JB, Schultz G, Burrell R, Nadworny P. Microbial biofilms and chronic wounds. Microorganisms. 2017;5:9. https://doi.org/10.3390/MICROORGANISMS5010009.
6. James GA, Swogger E, Wolcott R, Pulcini ED, Secor P, Sestrich J, Costerton JW, Stewart PS. Biofilms in chronic wounds. Wound Repair and Regeneration. 2008;16:37–44. https://doi.org/10.1111/J.1524-475X.2007.00321.X.
7. Shumba P, Shambat SM, Siemens N. The role of streptococcal and staphylococcal exotoxins and proteases in human necrotizing soft tissue infections. Toxins. 2019;11:332. https://doi.org/10.3390/TOXINS11060332.
8. Browne K, Chakraborty S, Chen R, Willcox MDP, Black DS, Walsh WR, Kumar N. (2020) A new era of antibiotics: The clinical potential of antimicrobial peptides. Int J Mol Sci. 2020;21(7047):21. https://doi.org/10.3390/IJMS21197047.
9. Lopes BS, Hanafiah A, Nachimuthu R, Muthupandian S, MdNesran ZN, Patil S. The role of antimicrobial peptides as antimicrobial and antibiofilm agents in tackling the silent pandemic of antimicrobial resistance. Molecules. 2022;27:2995. https://doi.org/10.3390/molecules27092995.
10. Silva JP, Appelberg R, Gama FM. Antimicrobial peptides as novel anti-tuberculosis therapeutics. Biotechnol Adv. 2016;34:924–40. https://doi.org/10.1016/j.biotechadv.2016.05.007.
11. Geitani R, AyoubMoubareck C, Touqui L, KaramSarkis D. Cationic antimicrobial peptides: alternatives and/or adjuvants to antibiotics active against methicillin-resistant Staphylococcus aureus and multidrug-resistant Pseudomonas aeruginosa. BMC Microbiol. 2019;19:54. https://doi.org/10.1186/s12866-019-1416-8.
12. Lin Z, Wu T, Wang W, Li B, Wang M, Chen L, Xia H, Zhang T. Biofunctions of antimicrobial peptide-conjugated alginate/hyaluronic acid/collagen wound dressings promote wound healing of a mixed-bacteria-infected wound. Int J Biol Macromol. 2019;140:330–42. https://doi.org/10.1016/j.ijbiomac.2019.08.087.
13. Dürr UHN, Sudheendra US, Ramamoorthy A. LL-37, the only human member of the cathelicidin family of antimicrobial peptides, Biochimica et Biophysica Acta (BBA). Biomembranes. 2006;1758:1408–25. https://doi.org/10.1016/j.bbamem.2006.03.030.
14. Yang B, Good D, Mosaiab T, Liu W, Ni G, Kaur J, Liu X, Jessop C, Yang L, Fadhil R, Yi Z, Wei MQ. Significance of LL-37 on immunomodulation and disease outcome. Biomed Res Int. 2020;2020:8349712. https://doi.org/10.1155/2020/8349712.

15. Rippon MG, Westgate S, Rogers AA. Implications of endotoxins in wound healing: a narrative review. J Wound Care. 2022;31:380–92. https://doi.org/10.12968/jowc.2022.31.5.380.
16. Osmokrovic A, Jancic I, Vunduk J, Petrovic P, Milenkovic M, Obradovic B. Achieving high antimicrobial activity: Composite alginate hydrogel beads releasing activated charcoal with an immobilized active agent. Carbohydr Polym. 2018;196:279–88. https://doi.org/10.1016/j.carbpol.2018.05.045.
17. Chereddy KK, Her C-H, Comune M, Moia C, Lopes A, Porporato PE, Vanacker J, Lam MC, Steinstraesser L, Sonveaux P, Zhu H, Ferreira LS, Vandermeulen G, Préat V. PLGA nanoparticles loaded with host defense peptide LL37 promote wound healing. J Contr Release. 2014;194:138–47. https://doi.org/10.1016/j.jconrel.2014.08.016.
18. Thoniyot P, Tan MJ, Karim AA, Young DJ, Loh XJ. Nanoparticle-hydrogel composites: concept, design, and applications of these promising, multi-functional materials. Adv Sci (Weinh). 2015;2(1–2):1400010. https://doi.org/10.1002/advs.201400010.
19. Puvirajesinghe TM, Zhi ZL, Craster RV, Guenneau S. Tailoring drug release rates in hydrogel-based therapeutic delivery applications using graphene oxide. J R Soc Interface. 2018;15:20170949. https://doi.org/10.1098/rsif.2017.0949.
20. Chen XY, Butt AM, Mohd Amin MCI. Enhanced paracellular delivery of vaccine by hydrogel microparticles-mediated reversible tight junction opening for effective oral immunization. J Contr Release. 2019;311–312:50–64. https://doi.org/10.1016/j.jconrel.2019.08.031.
21. Bhatnagar P, Law JX, Ng SF. Chitosan reinforced with kenaf nanocrystalline cellulose as an effective carrier for the delivery of platelet lysate in the acceleration of wound healing. Polymers. 2021;4392(13):4392. https://doi.org/10.3390/POLYM13244392.
22. Jacob B, Park I-S, Bang J-K, Shin SY. Short KR-12 analogs designed from human cathelicidin LL-37 possessing both antimicrobial and antiendotoxic activities without mammalian cell toxicity. J Peptide Sci. 2013;19:700–7. https://doi.org/10.1002/psc.2552.
23. Liang C-C, Park AY, Guan J-L. In vitro scratch assay: a convenient and inexpensive method for analysis of cell migration in vitro. Nat Protoc. 2007;2:329–33. https://doi.org/10.1038/nprot.2007.30.
24. Machado HA, Abercrombie JJ, You T, DeLuca PP, Leung KP. Release of a wound-healing agent from PLGA microspheres in a thermosensitive gel. Biomed Res Int. 2013;2013:387863. https://doi.org/10.1155/2013/387863.
25. Ali NH, Amin MCIM, Ng S-F. Sodium carboxymethyl cellulose hydrogels containing reduced graphene oxide (rGO) as a functional antibiofilm wound dressing. J Biomater Sci Polym Ed. 2019;30:629–45. https://doi.org/10.1080/09205063.2019.1595892.
26. Chereddy KK, Lopes A, Koussoroplis S, Payen V, Moia C, Zhu H, Sonveaux P, Carmeliet P, Rieux A, Vandermeulen G, Préat V. Combined effects of PLGA and vascular endothelial growth factor promote the healing of non-diabetic and diabetic wounds. Nanomedicine. 2015;11:1975–84. https://doi.org/10.1016/j.nano.2015.07.006.
27. McClements DJ. Encapsulation, protection, and delivery of bioactive proteins and peptides using nanoparticle and microparticle systems: A review. Adv Colloid Interface Sci. 2018;253:1–22. https://doi.org/10.1016/j.cis.2018.02.002.
28. Feczkó T, Tóth J, Dósa GY, Gyenis J. Optimization of protein encapsulation in PLGA nanoparticles. Chem Eng Process Process Intens. 2011;50:757–65. https://doi.org/10.1016/j.cep.2011.06.008.
29. Lozeau LD, Grosha J, Smith IM, Stewart EJ, Camesano TA, Rolle MW. Alginate affects bioactivity of chimeric collagen binding LL37 antimicrobial peptides adsorbed to collagen-alginate wound dressings. ACS Biomater Sci Eng. 2020;6(6):3398–410. https://doi.org/10.1021/acsbiomaterials.0c00227.
30. Toppazzini M, Coslovi A, Boschelle M, Marsich E, Benincasa M, Gennaro R, et al. Can the interaction between the antimicrobial peptide LL-37 and alginate be exploited for the formulation of new biomaterials with antimicrobial properties? Carbohydr Polym. 2011;83(2):578–85. https://doi.org/10.1016/j.carbpol.2010.08.020.
31. Zarzycki R, Modrzejewska Z, Nawrotek K. Drug release from hydrogel matrices. Ecol Chem Eng S. 2010;17(2):117–36.
32. Nicolle L, Journot CMA, Gerber-Lemaire S. Chitosan functionalization: Covalent and non-covalent interactions and their characterization. Polymers (Basel). 2021;13(23):4118. https://doi.org/10.3390/polym13234118.
33. Dong L, Henderson A, Field C. Antimicrobial activity of single-walled carbon nanotubes suspended in different surfactants. J Nanotechnol. 2012;2012:928924. https://doi.org/10.1155/2012/928924.
34. Szymańska E, Winnicka K. Stability of chitosan—a challenge for pharmaceutical and biomedical applications. Mar Drugs. 2015;13:1819–46. https://doi.org/10.3390/md13041819.
35. Quesada HB, de Araújo TP, Vareschini DT, de Barros MASD, Gomes RG, Bergamasco R. Chitosan, alginate and other macromolecules as activated carbon immobilizing agents: A review on composite adsorbents for the removal of water contaminants. Int J Biol Macromol. 2020;164:2535–49. https://doi.org/10.1016/j.ijbiomac.2020.08.118.
36. Sidik AM, Othaman R, Anuar FH. The effect of molecular weight on the surface and permeation of poly(L-lactic acid)-poly(ethylene glycol) membrane with activated carbon filler. Sains Malays. 2018;47:1181–7.
37. Xu K, An N, Zhang H, Zhang Q, Zhang K, Hu X, Wu Y, Wu F, Xiao J, Zhang H, Peng R, Li H, Jia C. Sustained-release of PDGF from PLGA microsphere embedded thermo-sensitive hydrogel promoting wound healing by inhibiting autophagy. J Drug Deliv Sci Technol. 2020;55:101405. https://doi.org/10.1016/j.jddst.2019.101405.
38. Bernal-Chávez SA, Alcalá-Alcalá S, Cerecedo D, Ganem-Rondero A. Platelet lysate-loaded PLGA nanoparticles in a thermoresponsive hydrogel intended for the treatment of wounds. Eur J Pharm Sci. 2020;146:105231. https://doi.org/10.1016/j.ejps.2020.105231.
39. Yoo J, Won Y-Y. Phenomenology of the initial burst release of drugs from PLGA microparticles. ACS Biomater Sci Eng. 2020;6:6053–62. https://doi.org/10.1021/acsbiomaterials.0c01228.
40. Kaur T, Thirugnanam A. Effect of porous activated charcoal reinforcement on mechanical and in-vitro biological properties of polyvinyl alcohol composite scaffolds. J Mater Sci Technol. 2017;33:734–43. https://doi.org/10.1016/j.jmst.2016.06.020.
41. Nagant C, Pitts B, Nazmi K, Vandenbranden M, Bolscher JG, Stewart PS, Dehaye J-P. Identification of peptides derived from the human antimicrobial peptide LL-37 active against biofilms formed by pseudomonas aeruginosa using a library of truncated fragments. Antimicrob Agents Chemother. 2012;56:5698–708. https://doi.org/10.1128/aac.00918-12.
42. Morgera F, Vaccari L, Antcheva N, Scaini D, Pacor S, Tossi A. Primate cathelicidin orthologues display different structures and membrane interactions. Biochemical Journal. 2009;417:727–35. https://doi.org/10.1042/BJ20081726.
43. El Maguana Y, Elhadiri N, Bouchdoug M, Benchanaa M, Jaouad A. Activated carbon from prickly pear seed cake: Optimization of preparation conditions using experimental design and its application in dye removal. Int J Chem Eng. 2019;2019:8621951. https://doi.org/10.1155/2019/8621951.
44. Rosenfeld Y, Papo N, Shai Y. Endotoxin (Lipopolysaccharide) neutralization by innate immunity host-defense peptides: Peptide properties and plausible modes of action. J Biol Chem. 2006;281:1636–43. https://doi.org/10.1074/jbc.M504327200.
45. Cirioni O, Giacometti A, Ghiselli R, Bergnach C, Orlando F, Silvestri C, Mocchegiani F, Licci A, Skerlavaj B, Rocchi M, Saba

V, Zanetti M, Scalise G. LL-37 protects rats against lethal sepsis caused by gram-negative bacteria. Antimicrob Agents Chemother. 2006; 50(5):1672–9. https://doi.org/10.1128/aac.50.5.1672-1679.2006.
46. Illsley MJ, Akhmetova A, Bowyer C, Nurgozhin T, Mikhalovsky SV, Farrer J, Dubruel P, Allan IU. Activated carbon-plasticised agarose composite films for the adsorption of thiol as a model of wound malodour. J Mater Sci Mater Med. 2017;28:154. https://doi.org/10.1007/s10856-017-5964-x.
47. Müller G, Winkler Y, Kramer A. Antibacterial activity and endotoxin-binding capacity of actisorb® silver 220. J Hospital Infect. 2003;53:211–4. https://doi.org/10.1053/jhin.2002.1369.
48. Tomasinsig L, Pizzirani C, Skerlavaj B, Pellegatti P, Gulinelli S, Tossi A, Di Virgilio F, Zanetti M. The human cathelicidin LL-37 modulates the activities of the P2X7 receptor in a structure-dependent manner. J Biol Chem. 2008;283:30471–81. https://doi.org/10.1074/jbc.M802185200.
49. Oudhoff MJ, Blaauboer ME, Nazmi K, Scheres N, Bolscher JGM, Veerman ECI. The role of salivary histatin and the human cathelicidin LL-37 in wound healing and innate immunity. Biol Chem. 2010;391:541–8. https://doi.org/10.1515/bc.2010.057.
50. Howling GI, Dettmar PW, Goddard PA, Hampson FC, Dornish M, Wood EJ. The effect of chitin and chitosan on the proliferation of human skin fibroblasts and keratinocytes *in vitro*. Biomaterials. 2001;22:2959–66. https://doi.org/10.1016/S0142-9612(01)00042-4.
51. Barańska-Rybak W, Sonesson A, Nowicki R, Schmidtchen A. Glycosaminoglycans inhibit the antibacterial activity of LL-37 in biological fluids. J Antimicrob Chemother. 2006;57:260–5. https://doi.org/10.1093/jac/dki460.
52. Ridyard KE, Overhage J. The potential of human peptide LL-37 as an antimicrobial and anti-biofilm agent. Antibiotics. 2021;10:650. https://doi.org/10.3390/antibiotics10060650.
53. Ke C-L, Deng F-S, Chuang C-Y, Lin C-H. Antimicrobial actions and applications of chitosan. Polymers (Basel). 2021;13:905. https://doi.org/10.3390/polym13060904.
54. Voljč T, Semenič D. Contribution of topical agents to wound healing. In: S. Aghaei (Ed.), Recent Advances in Wound Healing, IntechOpen, Rijeka, 2021: p Ch. 10. https://doi.org/10.5772/intechopen.97170.
55. Luo Y, McLean DTF, Linden GJ, McAuley DF, McMullan R, Lundy FT. The naturally occurring host defense peptide, LL-37, and its truncated mimetics KE-18 and KR-12 have selected biocidal and antibiofilm activities against candida albicans, staphylococcus aureus, and escherichia coli in vitro. Front Microbiol. 2017;8:544. https://doi.org/10.3389/fmicb.2017.00544.
56. Dean S, Bishop B, Van Hoek M. Susceptibility of pseudomonas aeruginosa biofilm to alpha-helical peptides: D-enantiomer of LL-37. Front Microbiol. 2011;2:128. https://doi.org/10.3389/fmicb.2011.00128.
57. Kang J, Dietz MJ, Li B. Antimicrobial peptide LL-37 is bactericidal against Staphylococcus aureus biofilms. PLoS ONE. 2019;14:e0216676. https://doi.org/10.1371/JOURNAL.PONE.0216676.
58. Overhage J, Campisano A, Bains M, Torfs EC, Rehm BH, Hancock RE. Human host defense peptide LL-37 prevents bacterial biofilm formation. Infect Immun. 2008;76(9):4176–82. https://doi.org/10.1128/iai.00318-08.
59. Kai-Larsen Y, Lüthje P, Chromek M, Peters V, Wang X, Holm Å, Kádas L, Hedlund KO, Johansson J, Chapman MR, Jacobson SH, Römling U, Agerberth B, Brauner A. Uropathogenic escherichia coli modulates immune responses and its curli fimbriae interact with the antimicrobial peptide LL-37. PLoS Pathog. 2010;6:e1001010. https://doi.org/10.1371/JOURNAL.PPAT.1001010.
60. Begun J, Gaiani JM, Rohde H, Mack D, Calderwood SB, Ausubel FM, Sifri CD. Staphylococcal biofilm exopolysaccharide protects against caenorhabditis elegans immune defenses. PLoS Pathog. 2007;3:e57. https://doi.org/10.1371/journal.ppat.0030057.